

# Electron Microscopic Study of Dehydration Transformations I. Twin Formation and Mosaic Structure in Hematite Derived from Goethite\*

FUMIO WATARI,† J. VAN LANDUYT, P. DELAVIGNETTE,‡  
AND S. AMELINCKX†

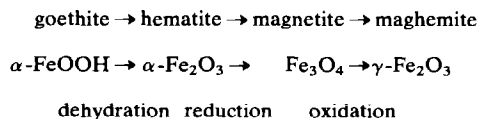
*University of Antwerp, RUCA, Groenenborgerlaan 171, B-2020 Antwerp,  
The Netherlands*

Received September 14, 1978

A study by means of electron microscopy at high resolution has enabled the analysis of the microstructure of hematite as produced by dehydration from goethite. The apparently "polycrystalline" structure is found to consist of aggregates of well-oriented twin-related hematite crystals, separated by regularly spaced H(001) walls of voids resulting from the loss of water. The material is thus broken up into blocks with sizes smaller than 50 Å. The crystallography of the twinned structure can be analyzed by electron diffraction data and dark-field imaging. These aggregates of hematite crystals provide an ideal mosaic structure. In particular the effect of this mosaic structure on the individual reflections of the diffraction patterns has been analyzed and discussed.

## 1. General Introduction

The goethite-hematite transformation is very important in the preparation process of materials for magnetic tape. This transformation proceeds in different stages which can be schematized as follows:



Throughout all these reactions the crystal habit is conserved. Such transformations are often termed "topotactic" (1). The first transformation is especially important since it influences the following reaction steps and determines to a large extent the characteristics of the final product.

\* Work performed under the auspices of the associations RUCA-SCK and ULB-IRE-CEN.

† Also at SCK-CEN, B-2400 Mol (Belgium).

‡ SCK-CEN, B-2400 Mol (Belgium).

It is well established that many hydroxides transform topotactically either into different hydroxides or into oxides (1-3). Two main groups of hydroxides can be distinguished: MOOH and M(OH)<sub>2</sub>. The hydroxides belonging to the type MOOH have in general several polymorphs; this is, for instance, the case for iron and aluminium hydroxides. Iron hydroxide occurs as goethite ( $\alpha$ -FeOOH) (4), akagenite ( $\beta$ -FeOOH) (5), lepidocrocite ( $\gamma$ -FeOOH) (6),  $\delta$ -FeOOH (7), and finally as a high-pressure form (8). Similar polymorphs occur in aluminium hydroxide, e.g., diasporite ( $\alpha$ -Al(OH)<sub>3</sub>) (4) and boemite ( $\gamma$ -Al(OH)<sub>3</sub>).

The dehydration process of these oxides has been studied previously; in particular a detailed study of the dehydration transformations of goethite into hematite and of diasporite into corundum was made by Lima de Faria (4). We shall briefly review this work, since our study is concerned with the same systems. Due to the increased

resolution of present-day electron microscopes we shall be able to study the transformation process *in situ* and in much greater detail. This series of papers also demonstrates the usefulness of high-resolution electron microscopy in the study of chemical reactions in general and of topotactic reactions in particular.

The study is divided into four parts. In Part I we discuss the microstructure of the hematite that results from dehydration of goethite. In Part II special attention will be devoted to the so-called "superstructure," whereas in Part III the mechanism of the transformation will be described. In Part IV the specific contribution of high-resolution electron microscopy to elucidating the mechanism will be described.

## 2. Summary of Previous Work

Lima de Faria studied the transformation by dehydration of goethite into hematite and of diaspore into corundum. Natural single crystals of these minerals were dehydrated by heating under vacuum, until pores were produced inside the specimen, and investigated in the course of the process by means of X-rays, electron microscopy, and thermogravimetry. A "superstructure" with a period of 32 Å in the goethite-hematite system and of 39 Å in the diaspore-corundum system was found, by means of X-rays as well as by means of electron microscopy.

In order to explain the dehydration process the existence of so-called donor and acceptor regions is postulated. Water molecules are formed in the donor regions as a result of the long-range diffusion of protons from the acceptor regions to the donor regions; the iron atoms diffuse in the opposite sense, i.e., from donor to acceptor regions.

The "superstructure" is formed as an intermediate state in which the iron concentration changes periodically in space; at the end of the process the superstructure disap-

pears and pores and oxide are formed. Such a mechanism is often termed "inhomogeneous nucleation and growth"; it was originally proposed by Ball and Taylor (9) for the case of brucite. In later investigations (10-12) the occurrence of a "superstructure" was not confirmed. The reason for this is rather trivial; in these later studies synthetic goethite was used instead of natural material. It turns out that the plate-shaped synthetic crystals are developed along (100), whereas the cleaved natural crystals are mostly parallel to (010) (13), which is the orientation that enables the "superstructure" to be observed. (See note added in proof.)

## 3. Introduction to Part I

It was suggested by Lima de Faria, on the basis of X-ray analysis, that hematite obtained by dehydration of single-crystal goethite was twinned (4). Although subsequently several attempts were made to study the transformation by direct observation using electron microscopy, it does not appear that the existence of twins in the hematite was proved, and the geometry of the twins has remained unknown (10-12). The reason for this will be clear from this paper. In the first place the observations have to be made along a suitable zone axis in order to reveal the twinned structure. Moreover just after the transformation the hematite occurs as very small crystals, of about 30-Å cross section, and very high resolution is required, especially since several crystals may overlap along the beam direction.

The small size of the hematite crystals affects the diffraction phenomena and, as will be shown in this paper, it allows one to study through electron diffraction the effect of the microstructure on the spot intensities. It is well known that in order to explain the intensities of different X-ray or neutron beams one has to assume that single crystals present a mosaic structure, i.e., the apparent single crystal is in fact composed of smaller

perfect blocks, to which the kinematical theory is applicable.

In electron diffraction, as a result of the much smaller wavelength, double diffraction occurs more easily and dynamical effects usually prevail. The actual block size of mosaic crystals usually exceeds the foil thickness. The hematite polycrystalline aggregates are quite unique in providing an opportunity to observe the onset of dynamical effects as the crystallites are made to grow in size. This peculiar texture of the hematite parts must be taken into account for a proper understanding of the observed diffraction effects and image characteristics, which are quite distinct from those due to single crystals.

In this first part we shall study in detail the particular texture of the hematite parts obtained from goethite single crystals by dehydration. Special attention will also be devoted to the diffraction effects and to the imaging effects due to this texture.

#### 4. Specimen Preparation

Although synthetic goethite has in general greater chemical purity than natural goethite, we decided to use mineral specimens because their crystal perfection is much better and larger specimens can be obtained by cleavage along different cleavage planes (13). The decomposition temperature of the natural material is somewhat higher than that of synthetic goethite i.e., 360°C against 280–320°C (14).

Synthetic goethite appears to be an aggregate of fine grains or needles (~50 to several hundred angstroms) as deduced from measurements of specific area (15) and from neutron diffraction (16). Its behavior with respect to the mechanism of dehydration may therefore be different from that of natural crystals. It was felt that natural crystals would be more suitable for a fundamental *in situ* study of the crystallography and the

mechanism of the process by means of high-resolution electron microscopy.

### 5. Observations

#### 5.1. Diffraction Patterns

In Fig. 1 we have reproduced three diffraction patterns with their zone axes along the [010] direction of goethite, which is parallel to the [010] direction of hematite of the same crystal area which has undergone dehydration. In Fig. 1a the crystal is still goethite, whereas in Fig. 1b the specimen is partly transformed into hematite. The transformation is completed in Fig. 1c. The indices of goethite and hematite spots are indicated in the schematic diffraction patterns of Fig. 1d. The diffraction pattern of Fig. 1c is that characteristic of a hexagonal single crystal, although it should be noted that hematite is rhombohedral (17).<sup>1</sup>

This diffraction pattern is in fact the superposition of two diffraction patterns due to the two types of rhombohedral hematite, obverse and reverse (18), in twin relationship. The spots belonging to the two components of this twin have been indicated with a different symbol in Fig. 1d. Note that a number of goethite spots coincide with hematite spots. In hematite no particular scattering halo is observed around the central spot, as is often the case in the diffraction pattern of crystals which have undergone a topotactic reaction.

The goethite spots are quite sharp in Fig. 1a, and there are no systematic intensity differences among the different spots although the corresponding extinction distances (indicated on the patterns) are significantly different. The hematite spots on the other hand are wide and somewhat diffuse in Fig. 1b; in Fig. 1c they have acquired satellites. Also, their intensities in Fig. 1c are different for a given component of

<sup>1</sup> The hexagonal three-indices system is used throughout.

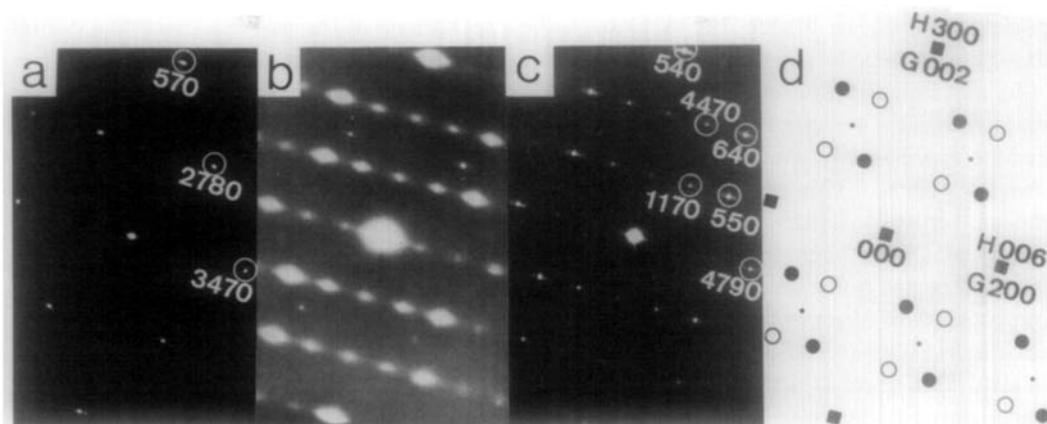


FIG. 1. Diffraction patterns of three stages of the goethite-hematite transformation. The patterns taken along the  $G[010]/H[010]$  zone are: (a) goethite; (b) the same area partly transformed; (c) the same area completely transformed to hematite; and (d) a schematic representation of the diffraction pattern, where: (•) goethite; (●) obverse hematite; (○) reverse hematite; (■) common to goethite and obverse and reverse hematite. In (a) and (c) the extinction distances are indicated next to the spot position.

the twin and are related to the corresponding extinction distances. Careful examination of the intensities of the spots reveals the following features.

(i) It is easy to distinguish intensity differences correlated with differences in the extinction distances among spots belonging to the pattern produced by one component of the hematite twins.

(ii) Even for spots common to both components of the hematite twins, intensity differences can be revealed, although not so easily.

(iii) There may be differences between intensities of homologous spots belonging to different components of the twin; however, these are small, suggesting that the volumes of the two components of the twin are very nearly equal.

(iv) The intensities of spots which are common to both components of the twin still present small differences among themselves as compared to the intensities of spots which belong to one component only; these are usually much stronger, which is consistent with the fact that now the whole volume of hematite contributes. In fact the common

spots are even stronger than one would expect from volume effect.

In goethite the intensities of the spots, especially of those close to the center, are very sensitive to the exact orientation of the specimen; this is much less the case in hematite, which seems to suggest that the nodes in reciprocal space are sharply defined in goethite, whereas they have become extended in hematite.

## 5.2. Images

Figure 2 shows the dark-field image of a specimen which has undergone transformation and further heat treatment; it has the orientation corresponding to the diffraction patterns of Fig. 1. The circle marked A in the inset shows the beams selected for the image. These belong to the two components of the twin, as is evident from the accompanying diagram. The image clearly shows two systems of one-dimensional fringes, parallel to  $H(\bar{1}02)$  and to  $H(102)$ , respectively, corresponding to the two components of the twin. The image thus reveals that the specimen is no longer a single crystal, but consists of small hematite

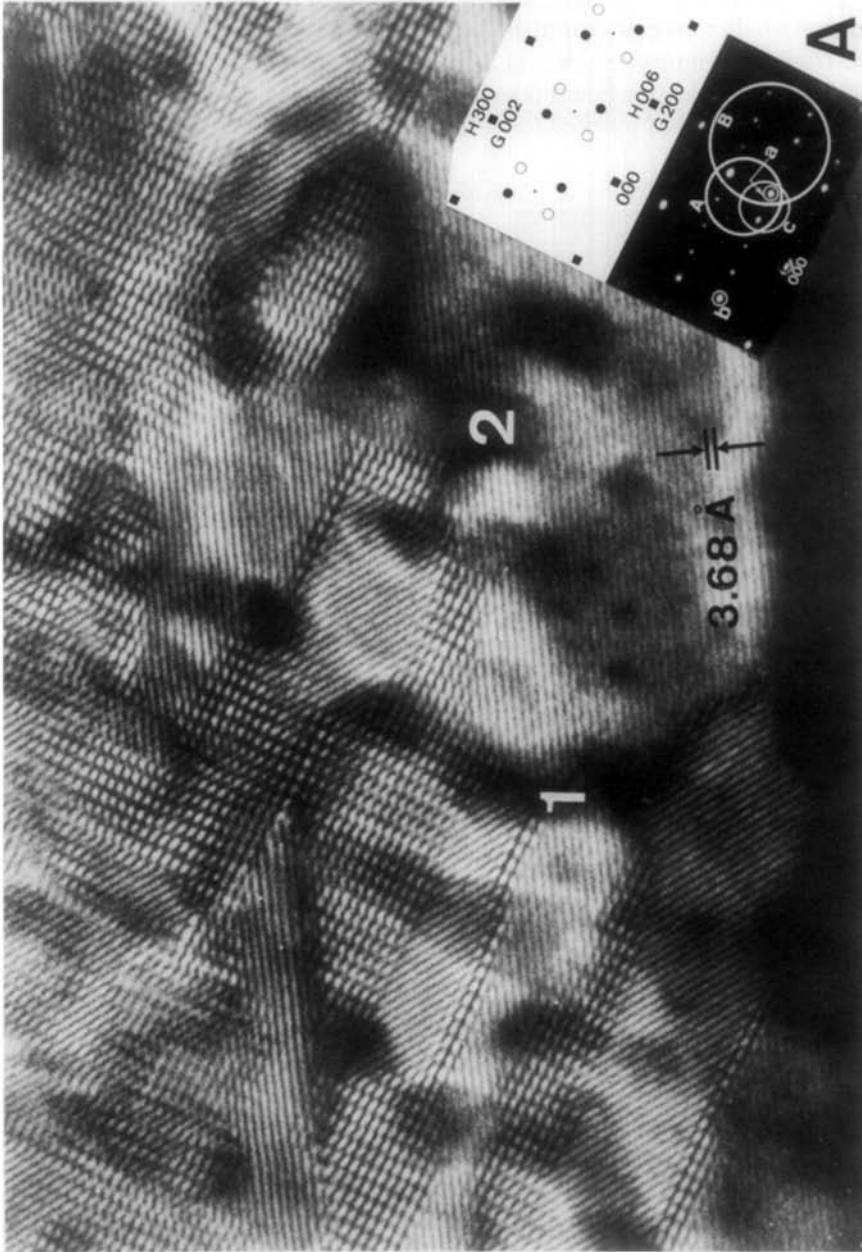


FIG. 2. Dark-field image of an area transformed into hematite after further heating. The image was obtained with the beams enclosed in circle A of the diffraction pattern, shown as an inset. Two systems of lattice fringes corresponding to  $H\bar{1}02$  and  $H(102)$  are closely resolved. The crystal is broken up into patches which are in twin relationship. The black part is void due to loss of water.

crystals, adopting two well-defined, twin-related orientations.

The "polycrystalline" multiply twinned nature of the specimen can best be appreciated at a somewhat smaller magnification, as in Fig. 3. The dark-field images shown in Figs. 3a–c were made by selecting beam (a), beam (b), and the pair of beams marked (c),

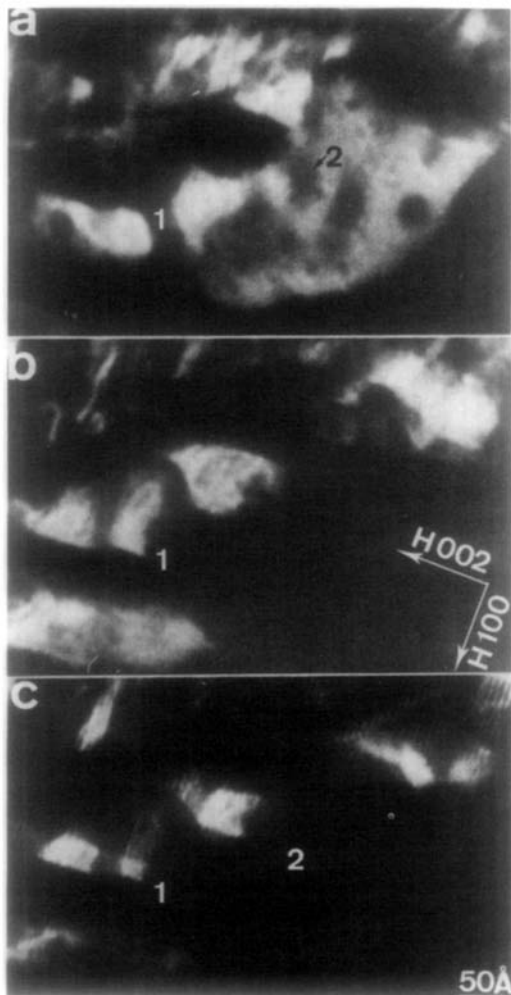


FIG. 3. Dark-field images obtained from beams (a), (b), and (c), respectively, marked on the inset of Fig. 2. Areas 1 and 2 in Fig. 2 are also indicated here for comparison. Images (a) and (b) are roughly complementary, whereas in (c) H(002) fringes appear only in the overlapping parts. The arrows in (b) indicate the directions of the diffraction vectors.

respectively, in the inset of Fig. 2. Points 1 and 2 in Figs. 2 and 3 indicate corresponding areas of the specimen. It is clear that the images shown in Figs. 3a and b are roughly complementary; the bright areas in Fig. 3a reveal one component of the twin, say the obverse part, and those in Fig. 3b the other component, i.e., the reverse part.

When two spots originating from differently oriented crystals are selected to produce the image as shown in (c) of the inset of Fig. 2, the corresponding dark-field image (Fig. 3c) exhibits H(002) lattice fringes. They only appear in the area where the two components of the twin overlap; this area corresponds with the area exhibiting mutually perpendicular crossed lattice fringes in Fig. 2.

In Fig. 2 the overlapping areas exhibit lattice fringes parallel to H(002) and to H(100); we shall see below how they originate. The H(100) plane often acts as a coherent twin plane, as is also visible in Fig. 2. Wavy fringes are due to local changes in thickness as a result of void formation and of overlap of crystals.

Figure 4 shows another aspect of the lattice fringes in area 1 in Fig. 2. The 2.70-Å fringes associated with the reflection H(104) reveal the twinned nature of the specimen. The 2.29-Å fringes on the other hand are common to both components. Note that these fringes, which are associated with the H(006) reflections, show a triple periodicity of weak fringes in the overlap area; this additional periodicity will be explained below.

The polycrystalline structure of hematite, resulting from the fine-scale twinning, markedly influences the lattice imaging. As we already noticed above, the twin can be distinguished in the  $G[010]/H[010]$  zone images. On the other hand, Fig. 5 was made from the same crystal part with zone axis parallel to H[151] or G[432]. In this specific orientation the diffraction pattern, shown as an inset, only exhibits spots due to one of the

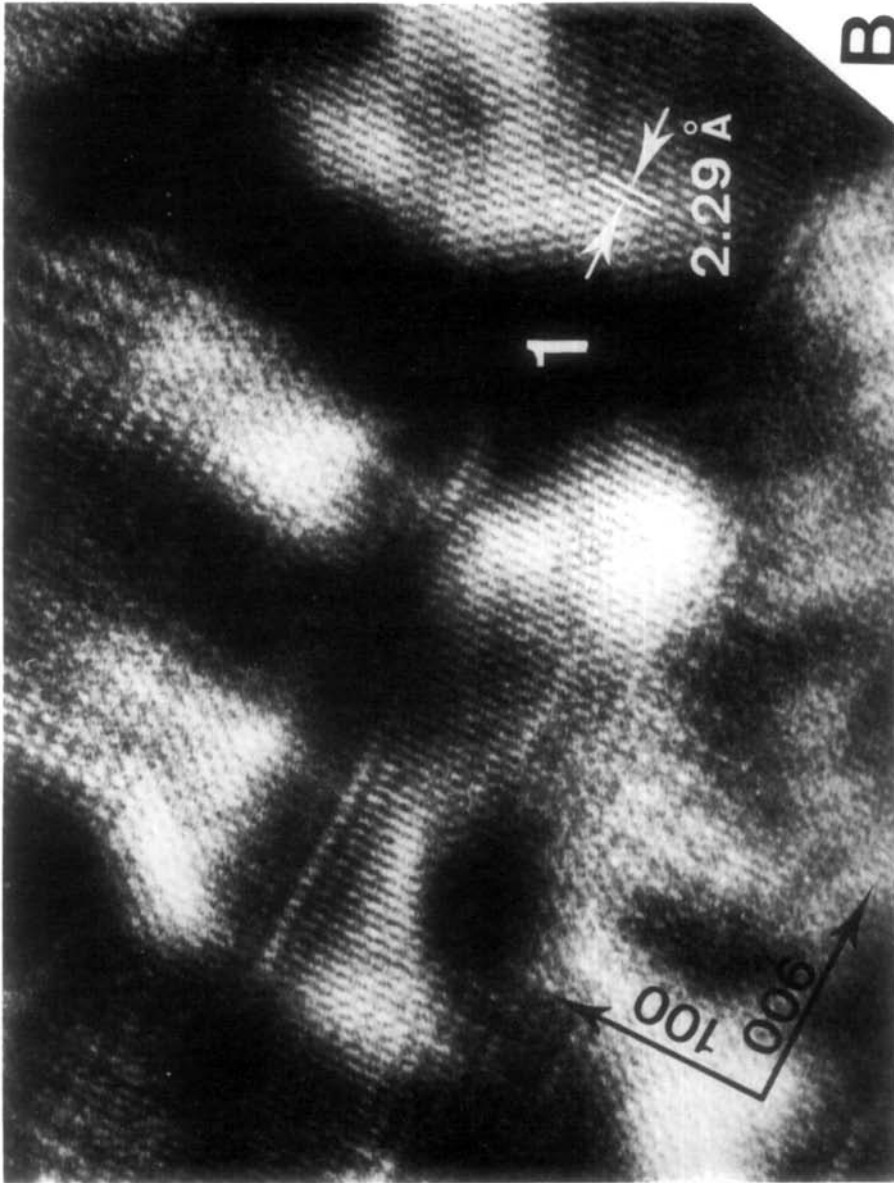


FIG. 4. Dark-field high-resolution image of area 1 in Fig. 2. The image was obtained from the reflections in circle B on the inset of Fig. 2. The H(104) and H(104) fringes reveal the twin relationship, and the H(006) fringe (2.29 Å) shows the plane common to both twin components. The diffraction vectors 100 and 001 are indicated by arrows.

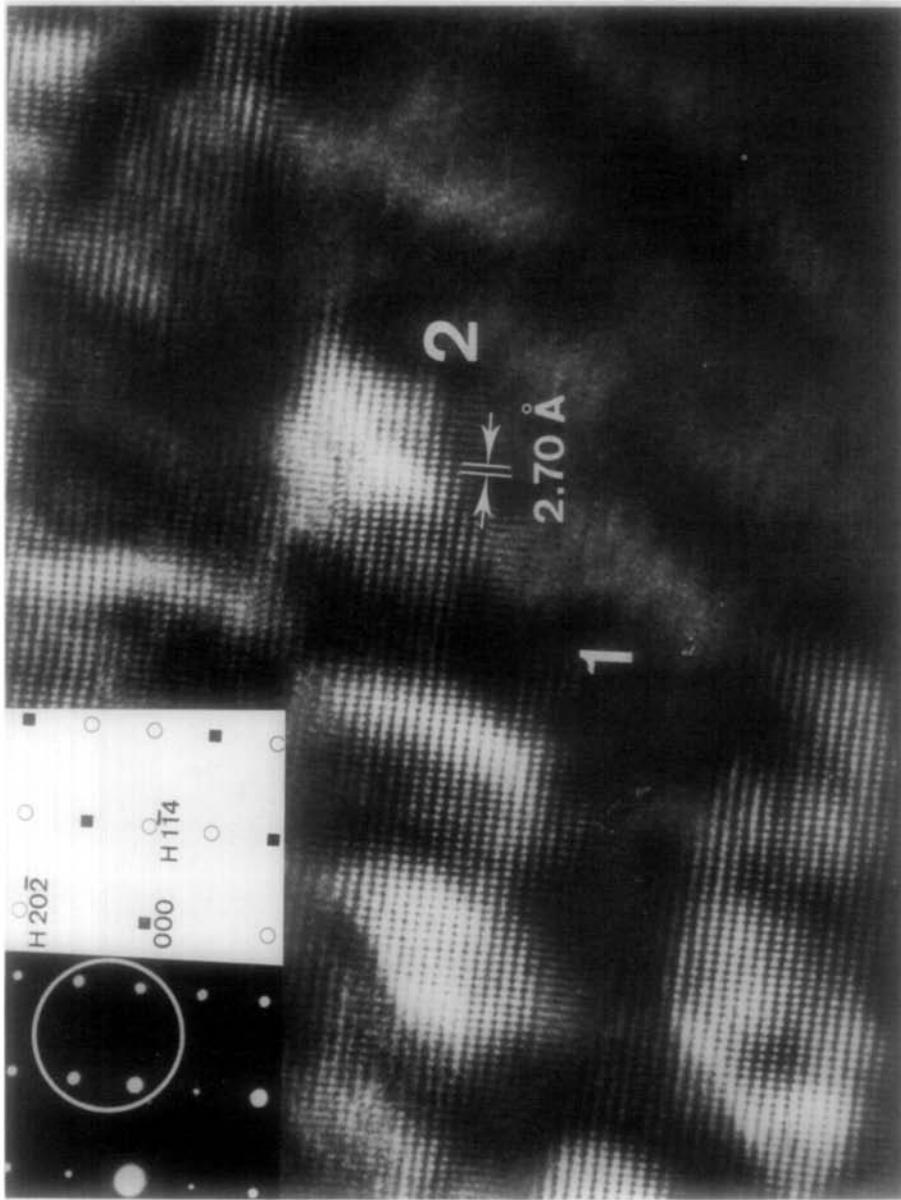


FIG. 5. Dark-field image of the same area as in Fig. 2 in an  $H[151]$  orientation. Regions 1 and 2 are indicated for comparison. The spots used for imaging are shown in the inset. Only the fringes corresponding to one variant are visible. Compare with Fig. 3c.



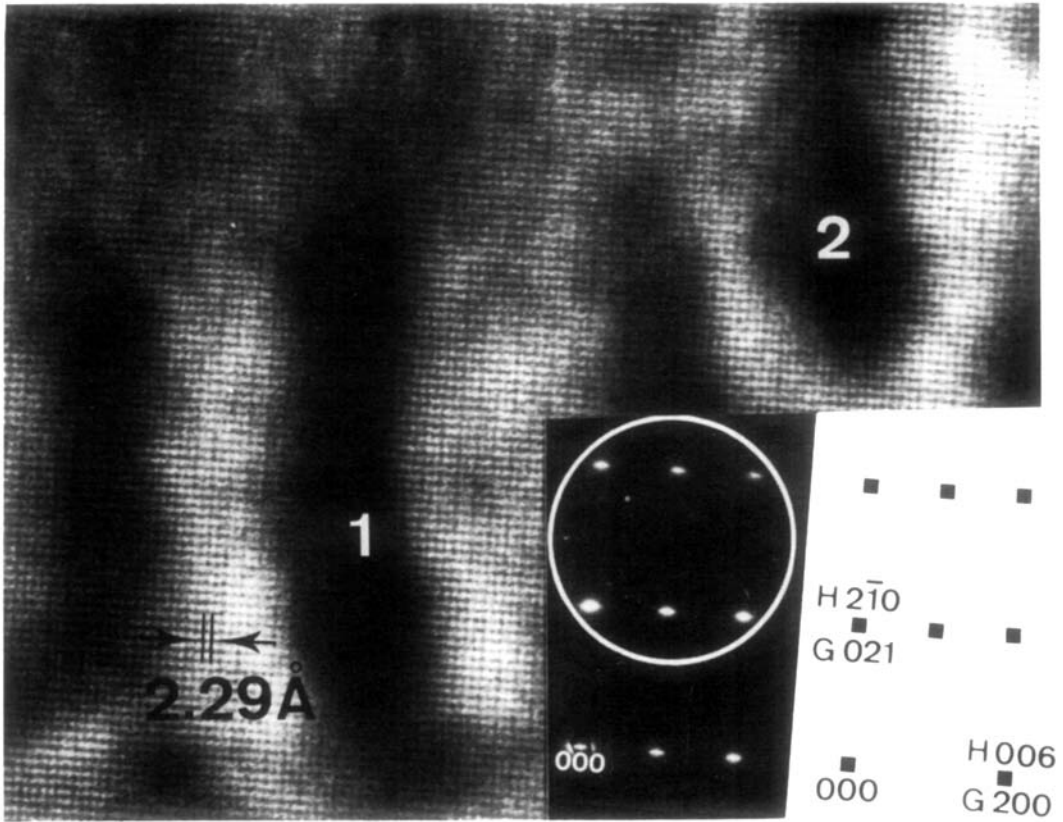


FIG. 6. Dark-field image of the same crystal part along the H[120] zone. Since this zone contains only spots which are common to both components no evidence for the twins is observed here.

two components of the twin, as well as spots which are common to both. Lattice fringes therefore only appear in the region of reverse crystal, as referred to in Fig. 3b.

Figure 6 was made parallel to zone H[120] which is also parallel to G[01 $\bar{2}$ ]. In this zone the diffraction pattern only exhibits spots which are common to both components of the twin. The resulting lattice fringes are quite continuous and there is no visible evidence for twinning, although the area contains several crystal parts in twin orientation as, e.g., near 1 and 2 on Fig. 2.

**6. Interpretation of the Observations**

*6.1. Structural Considerations*

The structure of goethite can best be described in terms of a hexagonally close-

packed array of oxygen atoms, which has AB stacking. The iron atoms occupy one-half of the octahedral interstices in this array in such a way that they form strips of two atom rows wide, as illustrated in Fig. 7a where the configuration of iron atoms projected on the basal plane of the oxygen lattice, that is, in G[100]/H[001] orientation, is shown (oxygen atoms are omitted, for clarity). The two positions of these strips (I and II) alternate with the periodicity of the HCP oxygen lattice so that the stacking symbol can be written as

$$\dots |A\gamma_I B\gamma_{II}| A\gamma_I B\gamma_{II} | \dots,$$

where  $\gamma$  represents the partially filled layers of metal ions in octahedral sites consisting of the above-mentioned strips.

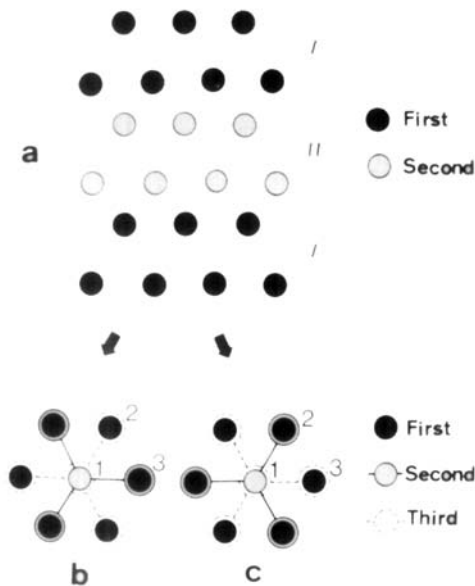
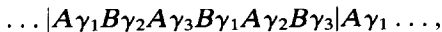


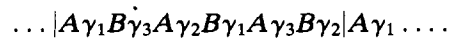
FIG. 7. Schematic representation of the iron configuration along the  $[100]$  direction for the goethite structure (a) and along the equivalent direction  $[001]$  for the two possible forms of the hematite structure (b and c). The projection plane is the basal plane of the common hexagonal close-packed oxygen lattice which is not drawn for clarity.

The structure of hematite is similarly based on a hexagonally close-packed array of oxygen atoms, in which the iron atoms now occupy two-thirds of the octahedral interstices, forming a hexagonal lattice with omissions akin to a honeycomb pattern. The omissions can occupy three possible positions (1, 2, and 3) of the hexagonal array of octahedral sites as shown in Figs. 7b and c. Whereas the stacking sequence of the oxygen along the  $c$ -axis of the hexagonal unit cell repeats after two layers the iron arrangement only repeats after three; as a result the complete sequence repeats after six layers only. This is evident from the layer notation which now becomes



where  $\gamma$  indicates the iron atoms in their octahedral sites and the subscript notes the position of the vacancies. The configuration

of iron atoms in the first half-unit cell is shown schematically in Figs. 7b and c. It can be seen that the succession of vacancies can form either a right-handed screw (Fig. 7b) where the first, second, and third layers are in positions 1, 2, and 3, respectively, or a left-handed screw as in Fig. 7c where the first, second, and third layers are in the positions 1, 3, and 2. The stacking symbol then becomes



These two possibilities give rise to the so-called obverse and reverse arrangements. Note that these two forms are related by a mirror operation. They have very approximately a common oxygen lattice, which is also common to goethite. The twinning clearly results from the different configurations of iron atoms occupying interstices in the same oxygen sublattice.

In order to account for the lattice images it is of interest to consider also the projections of the atomic structure along the  $H[010]/G[010]$  direction. In Fig. 8 we have represented such a projection for the obverse (a) and for the reverse (b) structures. The large circles represent oxygen atoms whereas the black and gray small circles represent iron atoms at two different levels. The two forms are obviously related by a mirror operation. In particular it is clear that the  $H(006)$  spacing is common to both, whereas the twinning is obvious from the  $H(102)$  and  $H(104)$  type planes. Figure 8c shows the configuration of iron atoms in crystal parts where obverse and reverse structures overlap. The diagram is obtained by the superposition of the configuration of iron atoms in Figs. 8a and b. It is now obvious that in the overlap image additional periods result such as  $H(100)$  and  $H(002)$ . The diagram of Fig. 8c has been made on the assumption that the oxygen lattice is continuous; this is not a requirement, however, for the generation of the additional periodicities. These diagrams can explain Fig. 2 and can be directly

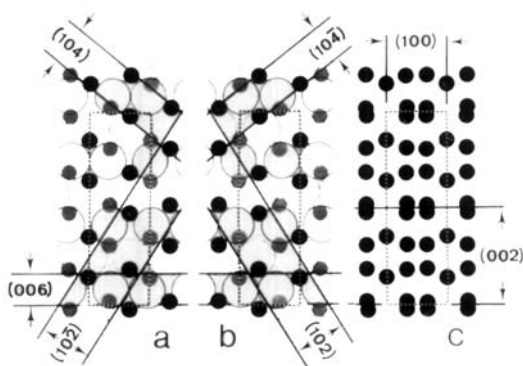


FIG. 8. H[010] projection of the structure where in (a) the obverse and in (b) the reverse structures are represented; (c) illustrates the configuration of iron atoms expected where obverse and reverse crystals overlap. The large circles in (a) and (b) represent the oxygen atoms.

compared with the lattice images of Fig. 4. The periodic contrast difference every third H(006) fringe in the region of overlap of Fig. 4 might well be due to this new period in the projected structure.

### 6.2. Textural Aspects

It is clear from the structural aspects of the transformation that the probabilities for nucleation of one or the other form of hematite from goethite must a priori be considered as equal. As a result the volumes of the two components of the twin are expected to be equal.

The shape of the hematite crystallites, due to the combined effect of dehydration and twinning, is approximately that of small blocks of 20- to 30-Å dimensions just after transformation. These are delimited by the H(001) void wall and by the perpendicular H(100) twin planes. After further heating some of the twins coalesce and give rise to larger crystallites of more than 50 Å in size. It was observed that immediately after the transformation, as well as after further heat treatment, the intensity ratio of the diffraction spots corresponding with the two variants remains close to unity. This is in

agreement with the equal probability of nucleation and with the fact that the configuration entropy is largest when obverse and reverse crystals with fixed size occupy the possible space equally and at random.

### 6.3. Diffraction Patterns

The relative spot sizes in goethite and hematite, as well as the different behaviors of the spot intensities in the two materials, can be understood by noting that goethite is a single crystal whereas hematite is a highly oriented aggregate of small twinned crystals. As a result, the dynamical theory should apply for goethite whereas the hematite parts would behave much more according to the kinematical theory of diffraction by a mosaic crystal.

The images have in fact shown that the hematite part consists of particles smaller than 50 Å but which are so highly oriented that they produce a single-crystal-like pattern.

The peculiar diffraction effects associated with the single-crystal goethite (case a), on the one hand, and with the highly twinned polycrystalline hematite that results from it, on the other hand (cases b and c), are summarized and illustrated in Table I.

The hematite specimens in fact exhibit a different mosaic structure for common reflections (case c) and for noncommon reflections (case b). The origin of the incoherency in the case of noncommon reflections is obviously the presence of the nonreflecting parts of the twins and of the voids. Apart from the fact that their presence determines the block size, the lattices of homologous parts of the twin aggregate on either side of the nonreflecting part may be slightly out of step and small orientation differences may also be present; both effects contribute to the mosaic spread.

For common reflections the noncoherency and the block size are mainly determined by the presence of the voids. The reflecting

TABLE I  
DIFFRACTION EFFECTS ASSOCIATED WITH SINGLE-CRYSTAL GOETHITE AND HIGHLY TWINNED POLYCRYSTALLINE HEMATITE

REAL SPACE <sup>(+)</sup>	RECIPROCAL SPACE <sup>(++)</sup>	DIFFRACTION DATA	CRYSTAL PROPERTIES
		<ul style="list-style-type: none"> <li>• sharp</li> <li>• sensitive</li> <li>• no evident relation</li> <li>• dynamical</li> <li>• coherent (single crystal)</li> <li>• well crystallized single crystal</li> </ul>	<ul style="list-style-type: none"> <li>• spot appearance</li> <li>• intensity variation for small orientation changes</li> <li>• intensity and structure amplitude</li> <li>• diffraction conditions</li> <li>• coherency for scattering (reason)</li> <li>• nature of crystal for diffraction</li> </ul>
		<ul style="list-style-type: none"> <li>• 3-dimensionally wide</li> <li>• not sensitive</li> <li>• directly related</li> <li>• kinematical</li> </ul>	<ul style="list-style-type: none"> <li>• apparent size as (b)</li> <li>• not sensitive</li> <li>• less obviously related</li> <li>• intermediate</li> <li>• less incoherent than (b) (voids, different configuration of Fe-atoms in twins)</li> <li>• less pronounced mosaic structure</li> </ul>

(+) (a), (b) and (c) are schematic images illustrating by hatching the crystal parts responsible for the spots marked (a), (b) and (c) res. in figure (d). The hatching also represents the lattice planes corresponding with these spots. (Inclination and spacing exaggerated).

(++) The crystal orientation is assumed to deviate from the exact zone axis.

(+++) The symbols for the spots are the same as in figure 1.

planes being continuous across the twin boundaries, the apparent crystallite size is larger and incoherency will mainly be caused by small differences in the deformation of the oxygen sublattices in the two parts of the twin due to the different orientations of the iron filling.

Other effects contributing to the mosaic spread of the hematite part and causing it to behave kinematically could be:

(i) Small misorientation due to the presence of voids. This effect seems to be smaller in the goethite-hematite system than in other topotactic systems.

(ii) Relaxation along the twin boundary.

(iii) The fact that the iron atoms do not adopt the ideal position in the centers of the oxygen octahedra, resulting in a different configuration of iron on both sides of the twin boundaries; this is, e.g., evident along the common H(006) planes in Figs. 8a and b.

## 7. Conclusion

Hematite produced by the dehydration reaction of single-crystal mineral goethite consists of highly oriented aggregates of small crystals less than 50 Å in size. The crystals are separated by arrays of voids, along H(001) planes; these result from the loss of water. High-resolution electron microscopy revealed the existence of twins and made it possible for their geometry to be determined; the H(100) plane is found to be the twin boundary.

The oxygen lattice is almost common to goethite and hematite; only the iron arrangements are different in the obverse and reverse hematite crystals. The volumes occupied by obverse and reverse crystals are approximately the same because the probabilities of formation are the same for both types of crystals; moreover it is expected that the configurational entropy is largest when obverse and reverse crystals occupy the available space equally and at random.

Although the lattice fringes are continuous in different crystals the polycrystalline-oriented aggregate behaves as an ideal mosaic crystal, since the kinematical theory of diffraction seems to be well satisfied.

Lattice imaging in such a highly oriented twinned polycrystalline aggregate allows one to perform novel types of contrast experiments. One can choose a particular orientation and a particular reflection in such a way as to reveal lattice fringes either in each part of the twin separately or in both regions simultaneously. Double diffraction allows one to reveal fringes with larger periods in overlapping twins.

Hematite obtained by the dehydration of goethite has an ideal mosaic structure in which the oxygen lattice is common and in which the incoherency is caused by the different configurations of iron atoms in the twin crystal and by the presence of void arrays along H(001) planes.

## 8. Acknowledgments

One of us (Fumio Watari) hereby acknowledges the fellowship awarded to him by the Belgian Ministry of National Education. He is also grateful to Dr. J. C. Mutin (University of Dijon, France) for useful discussions. The continued collaboration with M. Ghodsi and R. Derie (Services de Chimie Industrielle et de Chimie de Solides U.L.B., Bruxelles) is gratefully acknowledged.

*Note added in proof:* This phase transition was recently reexamined by a combination of differential thermal analysis, infrared spectroscopy, and electron microscopy techniques. (A. Lahousse, Thesis, ULB, Brussels). Mainly synthetic goethite powders but also mineral goethite were investigated. It was concluded that although the DTA-results revealed two endothermic peaks, the other techniques gave no evidence for the existence of an intermediate phase, although the electron microscopy observations confirmed by imaging and diffraction the typical aspects of a superstructure.

One of the authors (P.D.) then suggested that the superstructure might be a periodic succession of strips composed of hematite layers around a nucleus of goethite. The reasons for the nearly perfect periodicity of these strips were not clearly understood.

The present work was intended to elucidate the ambiguity in interpretation and to provide experimental evidence for a detailed model of this apparently complex phase transformation.

## References

1. J. R. GUNTER AND H. R. OSTWALD, *Bull. Inst. Chem. Res. Kyoto Univ.* **53**, 249 (1975).
2. D. R. DASGUPTA, *Indian J. Earth Sci.* **1**, 60 (1974).
3. H. MANSHAR, "Solid State Chemistry" (C. N. R. Rao, Ed.), p. 95, Dekker, New York (1974).
4. J. LIMA DE FARIA, *Z. Kristallogr.* **119**, 176 (1963).
5. I. DÉSZI, L. DESZTHELY, D. KULGAWCZUK, B. MCINAR, AND N. A. EISSA, *Phys. Status Solidi* **22**, 617 (1967).
6. R. GIOVANOLI AND R. BRÜTSCH, *Thermochim. Acta* **13**, 15 (1975).
7. W. FEITKNECHT, H. HÄNI, AND V. DVORAK, "Reactivity of Solids" (J. W. Mitchell *et al.*, Eds.), p. 237, Wiley, New York (1969).
8. M. PERNE, J. CHENAVAS, J. C. JOUBERT, C. MEYER, AND Y. GROSS, "*Solid State Commun.* **13**, 1147 (1973).
9. M. C. BALL AND H. F. W. TAYLOR, *Mining Mag.* **32**, 754 (1961).
10. Y. MAEDA, M. IGARASHI, A. TERADA, AND F. YOSHIMURA, *Japan. J. Appl. Phys.* **13**, 381 (1974).
11. W. VAN OOSTERHOUT, *Acta Crystallogr.* **13**, 932 (1960).
12. N. YAMAMOTO, T. SHINJO, M. KIYAMA, Y. BANDO, AND T. TAKADA, *J. Phys. Soc. Japan* **25**, 1267 (1968).
13. F. WATARI *et al.*, to be published.
14. I. DÉZSI AND M. FODOR, *Phys. Status Solidi* **15**, 247 (1966).
15. T. SHINJO, *J. Phys. Soc. Japan* **21**, 917 (1966).
16. A. SZYTULA *et al.*, *Phys. Status Solidi* **26**, 429 (1968).
17. R. W. G. WYCKOFF, "Crystal Structures," Interscience, New York, (1964).
18. N. F. M. HENRY AND K. LONSDALE, "International Tables for X-Ray Crystallography," Vol. 1, p. 20. The Kynoch Press, Birmingham, (1959).